applied sciences

MDPI

Article

Pneumatic Atomization: Beam-Steering Correction in Laser Diffraction Measurements of Spray Droplet Size Distributions

Marc O. Wittner *, Heike P. Karbstein and Volker Gaukel

Karlsruhe Institute of Technology, Institute of Process Engineering in Life Sciences, Chair of Food Process Engineering, Kaiserstrasse 12, 76131 Karlsruhe, Germany; heike.karbstein@kit.edu (H.P.K.); volker.gaukel@kit.edu (V.G.)

* Correspondence: marc.wittner@kit.edu; Tel.: +49-721-6084-8586

Received: 16 August 2018; Accepted: 25 September 2018; Published: 26 September 2018

Abstract: Laser diffraction is among the most widely used methods for spray droplet size measurements. However, the so-called beam-steering effect must be considered when pneumatic atomizers are used for droplet generation. The beam-steering effect is a systematic measurement error, leading to the detection of apparent large spray droplets due to gradients in the refractive index of the gas phase. The established correction method is based on the reduction of the laser diffraction system's measurement range by deactivation of detectors, relevant for the detection of large droplets. As this method is only applicable when size ranges of real and apparent droplet sizes are clearly different, an alternative method for beam-steering correction is introduced in the presented study. It is based on a multimodal log-normal fit of measured spray droplet sizes. The modality representing the largest droplets is correlated to the beam-steering effect and therefore excluded from the measured size distribution. The new method was successfully applied to previously published droplet size distribution measurements of an internal mixing Air-Core-Liquid-Ring (ACLR) atomizer. In measurements where the method of detector deactivation is applicable, excellent accordance of droplet size distributions, gained by both correction methods, was found. In measurements with overlapping real and apparent parts of the distribution, the new correction method led to a significant reduction of overestimated large droplets. As a consequence, we conclude that the new method presented here for beam-steering correction should be applied in laser diffraction measurements of spray droplet sizes, generated by pneumatic atomizers.

Keywords: beam-steering effect; laser diffraction; pneumatic atomization; ACLR; multimodal log-normal distribution

1. Introduction

Droplet size measurements of liquid sprays are an important tool for equipment and process design in many application areas, such as combustion technology, spray painting, or spray drying [1]. When rapid measurements of complete droplet size distributions are required, diffraction-based measurements are widely used [2]. This technique offers measurement of complete droplet size distributions with high measurement frequency [3]. However, in measurements of liquid sprays, the so-called beam-steering effect can lead to an overestimation of large droplets within the measured size distribution [4–6]. Beam steering occurs if the refractive index of the surrounding gas phase of the spray is not constant. As beam steering is a systematic error of laser diffraction measurements, the measurement principle is briefly described in the following section, before beam steering and its effect on droplet size measurements of sprays are described in more detail. For further information on laser diffraction measurements, a number of excellent reviews are available (e.g., [2,7]).

In laser diffraction measurements of sprays, the light of a laser beam is partly diffracted by droplets passing the beam. The diffraction caused by a single droplet is dependent on its size [8]. Small droplets diffract the light in larger angles, while larger droplets diffract the light in smaller angles. When a number of droplets pass the laser beam at the same time, a far-field Fraunhofer interference pattern of concentric rings is formed in the forward direction around the laser beam axis. A Fourier transform lens is used to focus the interference pattern onto a series of light-sensitive detectors, placed in defined distances around the central laser beam. Based on Fraunhofer diffraction theory, the droplet size distribution can be determined from the angular distribution of light intensity across these detectors [2]. In early laser diffraction instruments, each detector was directly associated with a specific droplet diameter interval. In modern laser diffraction spectroscopes, mathematical inversion procedures are used to calculate the volume-based droplet size distributions [3,7]. For this purpose, prediction models for the correlation between droplet size distributions and measured light energy distributions are used. These prediction models are based on mathematical probability functions to describe the relative frequency of dedicated droplet sizes within a distribution. However, each manufacturer uses different procedures and assumptions, which are considered as "know-how" and therefore are not made available to the user [7]. Nevertheless, the basic principles are the same in all cases. Besides Rosin-Rammler and Nukiyama-Tansawa distributions, log-normal distributions are the most common distribution functions used to describe droplet size distributions of spray measurements [9].

In a log-normal distribution, the logarithm of the droplet size $\ln(x)$ is normally distributed and can be described by the following function (1):

$$q(\ln(x)) = \frac{1}{x \cdot \sigma_{ln} \cdot \sqrt{2\pi}} exp\left\{ -\frac{(\ln(x) - \ln(x_{50}))^2}{2{\sigma_{ln}}^2} \right\} \quad (1)$$

In this function, x is the droplet size, x_{50} is the median of the distribution and σ_{ln} is the logarithmic standard deviation.

Multidisperse distributions, consisting of k modalities, can be described by the summation of k single log-normal distribution functions [10] according to Equation (2).

$$f(\ln(x)) = \sum_{1}^{k} A_k \cdot q_k(\ln(x)) \quad (2)$$

Here, A_k is the relative fraction of modality k, following the additional condition below (3).

$$\sum_{1}^{k} A_k = 1 \quad (3)$$

Recent instruments also include the Lorenz-Mie theory, which takes the contribution of small droplets to the angular light energy distribution by refraction into account [3]. When this contribution of light refraction is not considered and the corresponding portion of light is interpreted as diffracted light, small droplets are overestimated in the calculated size distribution.

Besides this, other systematic errors can affect laser diffraction measurements of liquid sprays, i.e., multiple scattering and beam steering. Multiple scattering can occur in optically dense sprays with transmission rates below 40% [3]. In this case, the laser beam may be diffracted by more than one particle before detection, leading to measurement errors. Beam steering can occur, when the refractive index in the gas phase is not constant. Local differences in the refractive index can be caused by different reasons. These may be concentration differences due to evaporation of the liquid phase, or density differences, due to gas compression or expansion and turbulent mixing of gas flows. When illuminated, differences in the refractive index of the gas phase lead to an additional low angle light scattering signal. In the field of flow visualization, this effect is known as "schlieren" and is used for the investigation of shock waves and other flow phenomena in transparent media [11,12]. However,

in laser diffraction measurements, this additional signal is interpreted as a droplet-caused scattering signal by the measurement system. As the low angle scattering signal mainly affects the measured light intensity on the inner detectors of the measurement device, the presence of large droplets is calculated by the mathematical inversion procedure [3–5].

The beam-steering effect must be considered, especially, when pneumatic atomizers are used. In pneumatic atomizers, the kinetic energy of compressed gas is used to deliver the necessary atomization energy. Expansion of the compressed atomization gas after leaving the nozzle leads to a significant decrease in density and therefore to a density gradient throughout the turbulently-mixed gas phase. In turn, this density gradient leads to a gradient in the refractive index of the gas phase. As gradients in density and therefore in refractive index increase with the pressure difference between compressed atomization gas and surrounding atmospheric gas, the beam-steering effect is especially observed at high input gas pressures [5].

When beam steering occurs, it is recommended both in the literature and by manufacturers of commercial measurement systems to deactivate the affected inner light detectors, correlated to the largest droplets [5,13]. This detector deactivation leads to a reduction of the system's measurement range. By this procedure, apparent droplets, caused by beam steering, are no longer detected by the laser diffraction system and therefore do not affect the measurement result. However, this method of beam-steering correction is only applicable when real and apparent parts of the droplet size distribution are clearly separated from each other.

But, when generated droplet sizes increase, the difference between the real and apparent part of the measured distribution gets smaller. From a certain point, both parts begin to overlap. In this case, it is no longer possible to find a measurement range that totally excludes the beam-steering effect from the measurement result, without excluding a part of the real droplet size distribution from the measurement result.

As a consequence, in practical measurements, a wider measurement range has to be accepted, when real and apparent distribution parts are not completely separated and the method of detector deactivation is applied. Although, this distribution still includes parts of the apparent droplet size distribution. This leads to a systematic overestimation of large droplets in the calculated size distribution. Hence, the characteristic value $x_{90,3}$, correlated to the largest droplets of a distribution, is scarcely used in the literature in the description of atomization results of pneumatic atomizers. For this purpose, typically, the Sauter mean diameter ($\overline{x}_{1,2}$) is used, as subsequent process steps (e.g., heat and mass transport) are mostly considered to be surface controlled [1]. Additionally, this value is more robust than $x_{90,3}$ against the described misbalance in droplet size distribution, caused by the beam-steering effect. This means the value of $\overline{x}_{1,2}$ varies little with changes in the largest droplet sizes, as the contribution of small droplets to the represented surface-to-volume ratio of a distribution is much higher.

However, especially when the largest droplets of a distribution have an over-proportional impact on the stability and performance of a subsequent process, this systematic overestimation of large droplets must be balanced, in order to present realistic values of $x_{90,3}$.

Therefore, a different approach for beam-steering correction of laser diffraction measurements is introduced in the presented study. This new correction method is based on the modification of the calculated droplet size distribution, instead of the modification of the measured light energy distribution by detector deactivation. It is based on a multimodal log-normal fit of measured spray droplet sizes. The modality representing the largest droplets is correlated to the beam-steering effect and therefore excluded from the measured size distribution. With this approach, contributions of real and apparent droplets can clearly be separated and the characteristic value $x_{90,3}$ can be determined without a systematic overestimation of large droplets. The new method is applied to previously published laser diffraction measurements of spray droplets, generated by a continuously working Air-Core-Liquid-Ring (ACLR) atomizer [14], which have until now solely been analyzed using the resulting $\overline{x}_{1,2}$ values. Results of the new correction method are compared to those corrected by detector

deactivation and values of measurements without correction. Although this new approach does not include final evidence by single droplet measurements, it follows the most probable interpretation of gained measurement results.

2. Materials and Methods

The correction method for spray droplet size distributions, presented in Section 3, will be applied to published droplet size measurements, generated by an ACLR atomizer [14]. For clarity, the used model system, spray test rig, and atomizer are described in the following sections. Furthermore, a gas capillary with variable exit diameter was used for investigation of the beam-steering effect, caused by the atomization gas expansion, without the impact of the liquid phase, see Section 2.3.

2.1. Model System

Aqueous solutions of maltodextrin (C*Dry MD01958, Overlack GmbH, Mönchengladbach, Germany) were used as a liquid model system for spray droplet size measurements. In order to ensure uniformity of the surface tension of all solutions, a concentration of 2% powdered whey protein concentrate WPC80 (Sachsenmilch GmbH, Leppersdorf, Germany) WPC80 was added. These solutions had a surface tension of 0.049 $N \cdot m^{-1}$. In Table 1, mean values and relative uncertainty values $u_r(\gamma)$ of the parameters viscosity (μ), surface tension (σ), density (ϱ), and refractive index (RI), as well as the total dry matter composition of the used solutions are summarized. All measurements were executed in triplicate at a temperature of 25 °C. In the rheological measurements, all solutions showed Newtonian behavior in the measurement range of shear rates between 1 and 1000 s^{-1}. Values of μ, given in Table 1, are measured at a shear rate of 1000 s^{-1}. For further information on model system characterization please refer to Wittner et al. [14].

Table 1. Physical properties of test solutions at 25 °C: viscosity (μ), surface tension (σ), density (ϱ), and refractive index (RI), as well as the corresponding uncertainty values $u_r(x)$ [14]. Concentrations of total dry matter c_{total}, Maltodextrin (c_{MD}), and WPC 80 ($c_{WPC\ 80}$) are given as dry base values (d.b.) in weight percent.

c_{total} (% d.b.)	$c_{WPC\ 80}$ (% d.b.)	c_{MD} (% d.b.)	μ (Pa·s)	$u_r(\mu)$ (%)	σ ($N \cdot m^{-1}$)	$u_r(\sigma)$ (%)	ϱ ($kg \cdot m^{-3}$)	$u_r(\varrho)$ (%)	RI (—)	u_r(RI) (%)
40	2	37	0.12	7.23	0.049	0.27	1185	0.74	1.404	0.08
47	2	45	0.39	4.61	0.049	1.03	1234	0.06	1.420	0.04
50	2	48	0.69	3.21	0.049	2.15	1240	0.48	1.427	0.03

2.2. Air-Core-Liquid-Ring (ACLR) Atomizer

In the ACLR atomizer, a gas capillary is used to inject a continuous gas core into the liquid stream, shortly before the exit orifice. The used capillary has an inner diameter ($d_{capillary}$) of 1.5 mm, leading to a gas injection area of 1.77 mm^2. The exit orifice length ($l_{exit\ orifice}$) and diameter ($d_{exit\ orifice}$) are 1.5 mm each. The mixing chamber length ($l_{mixing\ chamber}$) is 2.4 mm. This atomizer geometry was used previously by Stähle et al. [15,16], Kleinhans et al. [17,18], and Wittner et al. [14]. A scheme of the used ACLR atomizer is given in Figure 1.

2.3. Gas Capillary with Exchangeable Tip

For isolated investigations on the effect of atomization gas expansion on laser diffraction measurements by the beam-steering effect under process-like conditions, a modified gas capillary on the basis of the ACLR atomizer geometry was used. The gas capillary has a total length $l_{capillary\ mod}$ = 42.4 mm, consisting of the length of the capillary in the ACLR atomizer ($l_{capillary}$ = 40 mm) plus the length of the mixing chamber ($l_{mixing\ chamber}$ = 2.4 mm). The diameter is 1.5 mm. In the ACLR atomizer, the cross area of the exit orifice, occupied by the gas core, is reduced by the liquid lamella, due to the characteristic annular flow pattern. The thickness of the liquid lamella is dependent on product properties and applied process conditions. In order to mimic the gas core

in the ACLR atomizer under different flow conditions, the here-described modified capillary was equipped with three exchangeable tips (1.0, 1.3 and 1.5 mm). The length of the exit orifice was 1.5 mm, which is comparable to the used ACLR atomizer. A scheme of the used gas capillary is given in Figure 2.

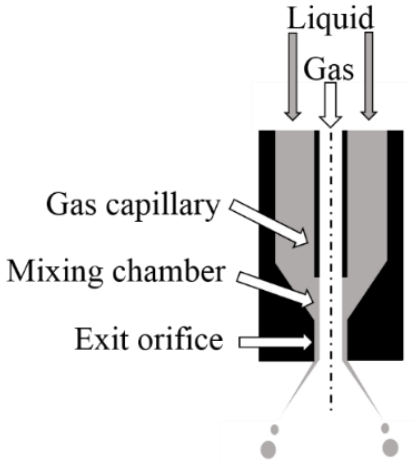

Figure 1. Scheme of the Air-Core-Liquid-Ring (ACLR) atomizer. ($d_{capillary}$ = 1.5 mm; $d_{exit\ orifice}$ = 1.5 mm; $l_{exit\ orifice}$ = 1.5 mm; $l_{mixing\ chamber}$ = 2.4 mm).

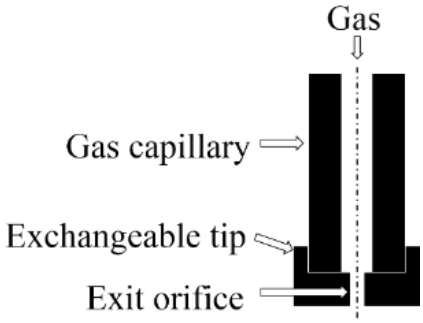

Figure 2. Scheme of the gas capillary ($d_{capillary}$ = 1.5 mm) with variable exit orifice diameter ($d_{exit\ orifice}$ = 1, 1.3, 1.5 mm; $l_{exit\ orifice}$ = 1.5 mm).

2.4. Spray Droplet Size Measurement by Laser Diffraction

A Malvern Spraytec laser diffraction spectrometer (Malvern Instruments, Malvern, UK) was used for spray droplet size measurements. It was equipped with a 750 mm focal lens, offering a droplet size measurement range of 2–2000 µm. Measurements were conducted at a frequency of 250 Hz over a time of 25 s, leading to the recording of 6250 droplet size distributions per measurement. Based on this data, an averaged droplet size distribution was calculated with consideration of the refractive indices of the used model solutions. As a reference procedure for beam-steering correction, all measurements were evaluated with the method of detector deactivation, as is recommended both in the literature [5] and by the manufacturer of the measurement device [13]. The device-specific software, Malvern Spraytec (v.3.30), was used for application of the detector deactivation procedure and for calculation of averaged droplet size distributions. In order to exclude the effect of multiple scattering on droplet size distribution measurements, transmission rates above 40% were ensured for all measurements [3].

2.5. Spray Test Rig

For spray characterization experiments a spray test rig was used. The solutions were supplied by an eccentric screw pump (MD 006-12, seepex GmbH, Bottrop, Germany) at a flow rate of 20 L/h. Compressed air for atomization was supplied by a compressor (Renner RSF-Top 7.5, Renner GmbH,

Güglingen, Germany) and dehumidified by a condenser (CQ 0065/1133A, Renner GmbH, Güglingen, Germany). Atomization gas pressures of 0.6 and 0.8 MPa were adjusted using a pressure regulator. Corresponding gas volume flows were measured by a gas flow meter (ifm SD6000, ifm electronic, Essen, Germany). As is typically executed in the literature (e.g., [1]), the atomization processes are characterized by the ratio between mass flow of the gas and liquid stream (gas to liquid ratio by mass, GLR). For spray droplet size measurements, the Malvern Spraytec laser diffraction spectroscope was mounted to the test rig. In spray droplet measurements, the laser beam crossed the full cone of the spray angle at the atomizer exit centerline at a vertical distance of 250 mm. The spray was collected in a vessel below the measurement zone. This vessel was connected to an exhaust fan. In the vessel, a filter was used to prevent recycling of small droplets back into the measurement zone. For investigation using the modified gas capillary, the vertical distance between the capillary tip and laser beam was reduced to 30 mm. In this case, gas pressures of 0.3, 0.6, and 0.9 MPa were applied. For the calculation of apparent droplet sizes from light scattering patterns, the refractive index of the model solution with 0.12 Pa·s (1.404) was used. This procedure was chosen as in real spray droplet size measurements the refractive index of the liquid is used for droplet size calculation.

2.6. Calculations and Statistical Analysis

OriginPro software, version 9.4 G (OriginLab Corporation, Northampton, USA) was used for calculation of fitting curves and statistical analysis. For fitting curves, the Levenberg Marquard iteration algorithm was used. As a goodness of fit parameter, the corrected determination coefficient R^2 was used. The effects of viscosity and the applied method for beam-steering correction on the characteristic values of droplet size distributions, as well as the effect of input parameters (p_{gas}, $d_{exit\ orifice}$) on apparent droplet size distributions were evaluated by a one-way analysis of variance (ANOVA). Scheffé's test was used for comparison of means. In the performed tests, a probability of $p < 0.05$ was used for the identification of significant differences.

3. Results and Discussion

3.1. Application and Limitations of the Detector Deactivation Method

In the following section, the method of beam-steering correction by detector deactivation is illustrated. Therefore, the measurement of droplet sizes generated by an internal mixing Air-Core-Liquid-Ring (ACLR) atomizer [14–18] is depicted in Figure 3A (μ = 0.12 Pa·s; p_G = 0.8 MPa; $\dot{V}_L$ = 20 L/h; GLR = 0.36). According to the form of the q_3-plot, with the characteristic gap between the real and apparent droplet size distribution, the measured signal on the inner detectors is solely caused by the beam-steering effect under these conditions [5]. When the corresponding detectors are deactivated (in this case detector 1–8), the mathematical inversion procedure calculates the particle size distribution, shown in Figure 1 (filled circles). As the detector deactivation simply results in a reduction of the instrument's measurement range, the corrected droplet size distribution shows the same form as when the beam-steering peak is manually cut off, and the remaining area under the curve is restandardized to a value of 1 (manual cut, Figure 1). It can be concluded that the method of detector inactivation does not change the properties of the real particle distribution if the real and apparent parts of the measured distribution are clearly separated. The method of manual distribution cutting is not usually performed as manipulation of the result of the measurement device is not preferred. However, detector deactivation essentially uses the same method.

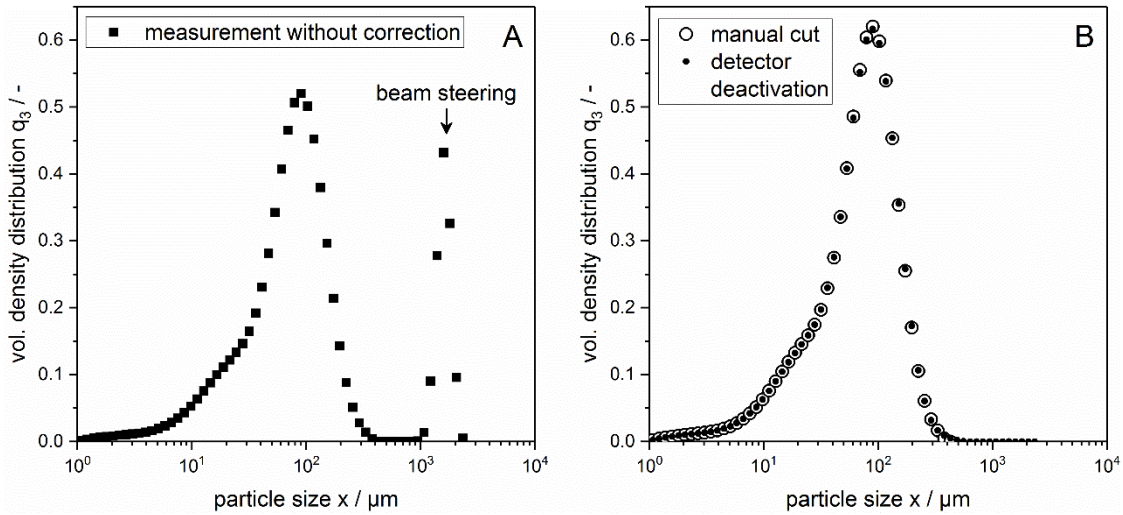

Figure 3. (**A**) Exemplary volumetric density distribution with beam-steering effect (µ = 0.12 Pa·s; p_G = 0.8 MPa; $\dot{V}_L$ = 20 L/h; GLR = 0.36). Real and apparent distribution parts are completely separated. (**B**) Distribution after beam-steering correction by distribution cutting (empty circles) and detector deactivation (filled circles).

When droplet sizes increase, the real and apparent parts of the distribution might not be completely separated in the plot of q_3, see example in Figure 4, although the beam-steering peak is clearly distinct in the given example (µ = 0.69 Pa·s; p_G = 0.8 MPa; $\dot{V}_L$ = 20 L/h; GLR = 0.35).

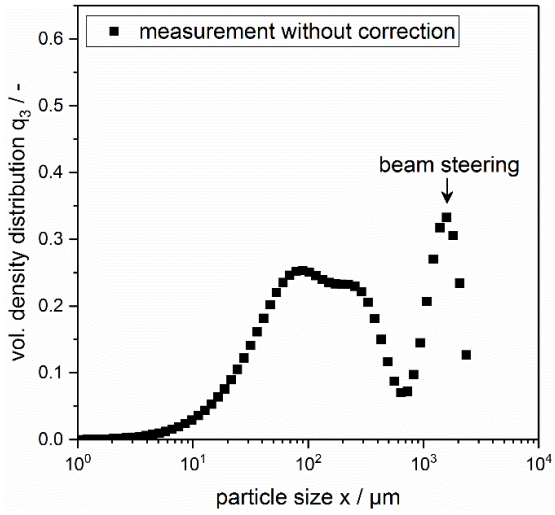

Figure 4. Exemplary volumetric density distribution with beam-steering effect (µ = 0.69 Pa·s; p_G = 0.8 MPa; $\dot{V}_L$ = 20 L/h; GLR = 0.35). The real and apparent distribution parts overlap. No beam-steering correction performed.

In this case, the signal measured by certain detectors is composed of light, diffracted by large particles and of light, scattered due to the beam-steering effect. It is not possible to determine the different fractions of light. If all affected detectors are deactivated, a portion of light would be cut off that is actually diffracted by existing large droplets. Additionally, it is not possible to clearly measure which detectors are solely affected by the beam-steering effect, making it even more difficult to decide how many detectors can be deactivated. Moreover, it is important to notice that the measurement range of the prediction model for the correlation between the light intensity measurement and corresponding droplet size distribution is not necessarily affected by detector deactivation. The depicted graph does not decrease to zero when the end of the measurement range is reached. It is noteworthy at this point,

that the measurement range is given as 2–2000 µm by the manufacturer for the used setup. However, the implemented mathematical inversion routine calculates droplet sizes up to 2500 µm, based on the underlying probability function which is defined to infinity, see Equation (2). This also means that when detectors are deactivated and the real distribution includes droplets with sizes near the maximum measurable size, it is possible that the calculated droplet size distribution will include droplets that are actually outside the instrument's reduced measurement range. These facts lead to the necessity of a different beam-steering correction method for use when real and apparent parts of the droplet size distribution overlap.

3.2. Influence of Processing Conditions on Apparent Spray Droplet Sizes

In order to apply a beam-steering correction by distribution fitting, the influence of the atomization process conditions on apparent droplet sizes must be investigated. Therefore, a special gas capillary with an exchangeable tip was used in the presented study, see Section 2.3. As an example, the measured volumetric density distribution q_3 of apparent droplet sizes are depicted in Figure 5 for measurements with an exit orifice diameter of 1.0 mm (1.5 mm) and a gas pressure of 0.3 MPa (0.9 MPa) on the left (right) side. Additionally, the corresponding log-normal fits ($R^2 > 0.99$) are shown. The parameters used were chosen as they represent the extrema of the applied process parameters. This means, the smallest exit orifice diameter at the lowest gas pressure (left) resulting in the smallest gas volume flow (0.7 $Nm^3 \cdot h^{-1} \pm 0.1$) and the largest exit orifice diameter at the highest gas pressure (right) resulting in the largest gas volume flow (8.2 $Nm^3 \cdot h^{-1} \pm 1.1$).

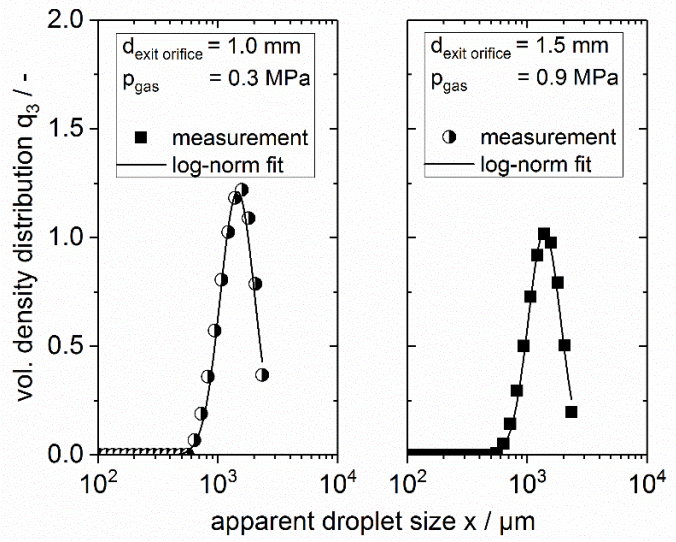

Figure 5. Volumetric density distribution q_3 of apparent droplet sizes ((**left**) $d_{exit\ orifice}$ = 1.0 mm, p_{gas} = 0.3 MPa; (**right**) $d_{exit\ orifice}$ = 1.5 mm, p_{gas} = 0.9 MPa) and corresponding log-normal fits ($R^2 > 0.99$).

The apparent droplet size distributions presented vary over a small range, concerning both form and position. Mean values and the corresponding uncertainty values $u_r(x)$ of $x_{10,3}$, $x_{50,3}$, $x_{90,3}$ are shown for measurements under the processing conditions presented in Table 2. The described behavior was found for all measurements ($d_{exit\ orifice}$ = 1.0, 1.3, 1.5 mm; p_{gas} = 0.3, 0.6, 0.9 MPa). Hence, all measured apparent droplet size distributions, caused by the beam-steering effect, could be fitted by a log-normal distribution curve with R^2 higher than 0.99. However, no significant influence of p_{gas} or $d_{exit\ orifice}$ on position and form of apparent droplet size distributions was found in the statistical analysis.

Table 2. Mean values and the corresponding uncertainty values $u_r(x)$ of $x_{10,3}$, $x_{50,3}$, $x_{90,3}$ for measurements of apparent droplet sizes, caused by beam steering.

$d_{exit\ orifice}$ (mm)	P_{gas} (MPa)	$x_{10,3}$ (µm)	$u_r(\mu)$ (%)	$x_{50,3}$ (µm)	$u_r(\sigma)$ (%)	$x_{90,3}$ (µm)	$u_r(\varrho)$ (%)
1	0.3	953	3.8	1448	1.34	2039	1.04
1.5	0.8	912	0.7	1381	0.59	1972	0.50

Although the measured distributions vary only in small ranges, the impact of the beam-steering effect cannot be generalized using a fit function with fixed coefficients. Based on these results, apparent droplet size distributions can be approximated by individual log-normal distribution fits. This might be different when higher gas pressure differences between inlet and atmospheric conditions are present, as gas expansion might have a more pronounced impact. This point should be investigated in further studies. Moreover, the presented study is performed with regard to continuously working atomizers. These atomizers are designed to deliver droplet size distributions of high temporal steadiness. Hence, apparent droplet size distributions also show highly constant values over time. When atomizers are operated in pulsed mode, like in discontinuous combustion applications, the positon and form of apparent droplet sizes may be changing over time. Hence, further studies may addressed the effect of beam steering under discontinuous operation conditions.

3.3. New Procedure for Beam-Steering Correction

In Figure 6, the new procedure for beam-steering correction in droplet size distributions is described. As an example, the drop size distribution measurement already depicted in Figure 4 (μ = 0.69 Pa·s; p_G = 0.8 MPa; $\dot{V}_L$ = 20 L/h; GLR = 0.35), was selected. The different steps are marked by the letters A–C.

(A) Firstly, a multimodal log-normal distribution (see Section 2.6) is fitted to the droplet size distribution, calculated by the mathematical inversion procedure of the measurement device. According to Equation (2), the method allows the application of an infinite number of modalities. However, as the number of fit parameters increases with the number of modalities, their amount should be reduced to a minimum value that still represents the full distribution sufficiently. In the presented study, trimodal log-normal fits are used for this purpose. Therefore, nine coefficients have to be fitted (x_{501-3}, σ_{1-3}, A_{1-3}). It must be mentioned that different multimodal probability functions, like Rosin-Rammler or Nukiyama-Tansawa, could deliver better results when other laser diffraction spectroscopes are used.

(B) The trimodal log-normal curve is split into its single modalities. The 3rd modality, representing the largest droplets, is considered to represent the apparent droplet size distribution caused by the beam steering effect (see Section 3.1).

(C) A modified distribution is formed by the combination of the 1st and 2nd modality to a bimodal log-normal distribution. The area under the curve (AUC) is re-standardized to a value of 1 by balancing the ratio indicators A_1 and A_2 in the following way:

$$A_{1;2\ mod} = \frac{A_{1;2}}{(1 - A_3)} \quad (2)$$

The results of all performed measurements were fitted by a trimodal log-normal distribution with R^2 values above 0.99. In this example, a measurement with overlapping real and apparent droplet size distributions was used, as in this case the standard procedure of detector deactivation cannot be applied. In Figure 7, uncorrected and modified distributions are compared to each other. The modified distribution is much narrower than that of the uncorrected measurement. The characteristic plateau, caused by the beam-steering effect, is successfully removed.

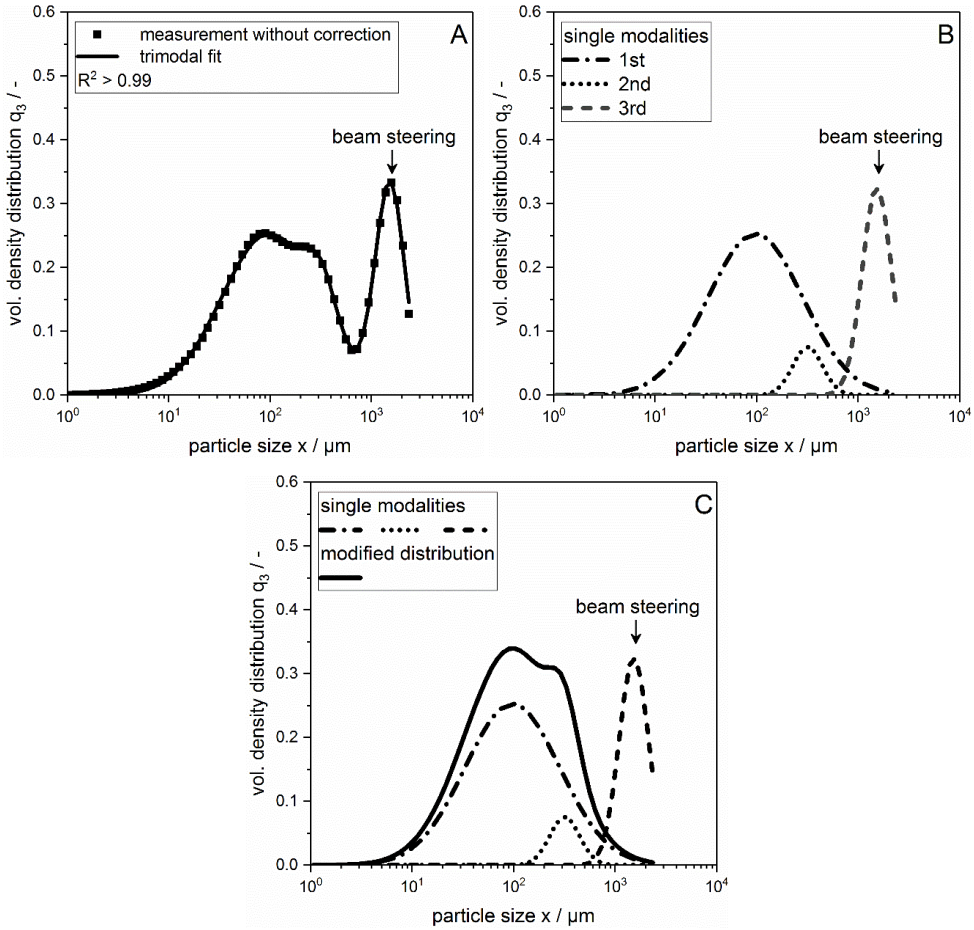

Figure 6. Procedure of beam-steering correction, exemplarily presented at a measurement with overlapping real and apparent droplet size distribution (µ = 0.69 Pa·s; p_G = 0.8 MPa; $\dot{V}_L$ = 20 L/h; GLR = 0.35): (**A**) Trimodal log-normal fit of the measured droplet size distribution. (**B**) Split in single modalities. (**C**) Formation of modified droplet size distribution.

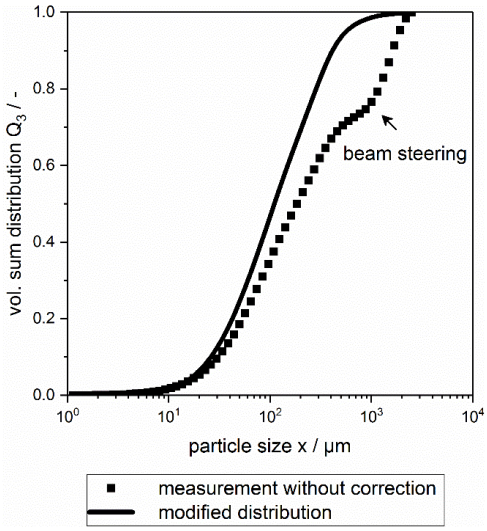

Figure 7. Comparison of uncorrected and modified distributions (µ = 0.69 Pa·s; p_G = 0.8 MPa; $\dot{V}_L$ = 20 L/h; GLR = 0.35).

Still, it must be ensured that the mode of the apparent droplet size distribution is detectable by the applied multimodal probability function. This means that the method cannot be applied when the

overlap of real and apparent droplet size distribution exceeds a certain extent. Moreover, the method does not include final evidence of exact droplet size distribution measurements. However, it delivers the most probable interpretation of gained measurement results when log-normal fits with R^2 values above 0.99 are applicable. For further validation, gained results could be compared to results of other measurement techniques, like shadowgraphic imaging or Phase Doppler Anemometry (PDA).

In order to show the applicability of the presented method for measurements where real and apparent droplet size distributions are completely separated, a measurement at low liquid viscosity (μ = 0.12 Pa·s) is shown in Figure 8. In addition to uncorrected (squares) and modified sum distributions (line), droplet size distributions corrected by detector deactivation (triangles, detectors 1–8 deactivated) and distribution cutting (circles) are depicted.

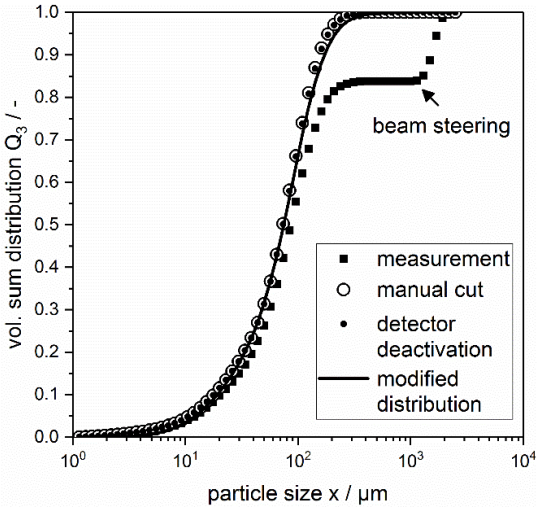

Figure 8. Comparison of beam-steering correction methods. Sum distributions of a measurement with low viscous medium (μ = 0.12 Pa·s, p_{gas} = 0.8 MPa). Uncorrected measurement (squares), correction by manual cutting (empty circles), correction by detector deactivation (filled circles), and correction by the new modification procedure described (line).

In the presented example, all three correction methods (detector deactivation, manual cutting, and the new modification procedure) are applicable, as real and apparent droplet size distributions do not overlap in the density distribution curve, see Figure 3A. All methods are capable of removing the beam-steering plateau from the measured droplet size distribution. The resulting corrected sum distributions show excellent agreement with each other in this example.

In Figure 9, characteristic values of droplet size distributions are shown for gas pressures p_{gas} of 0.6 MPa (left) and 0.8 MPa (right) and different liquid viscosities (0.12, 0.39, 0.69 Pa·s). As characteristic values of droplet size distributions, the percentiles $x_{10,3}$, $x_{50,3}$, $x_{90,3}$, and the sauter mean diameter ($\overline{x}_{1,2}$) are presented. Values of the measurement without correction are indicated by empty symbols. Values corrected by detector deactivation method are indicated by half-filled symbols. Values corrected by the new modification procedure are indicated by filled symbols. To improve the readability of the diagram, the so-called point shift technique is used. This means that data points are shifted around the given viscosities of 0.12, 0.39, and 0.69 Pa·s, respectively. Nevertheless, although they are shifted, the values in one group have the same viscosity.

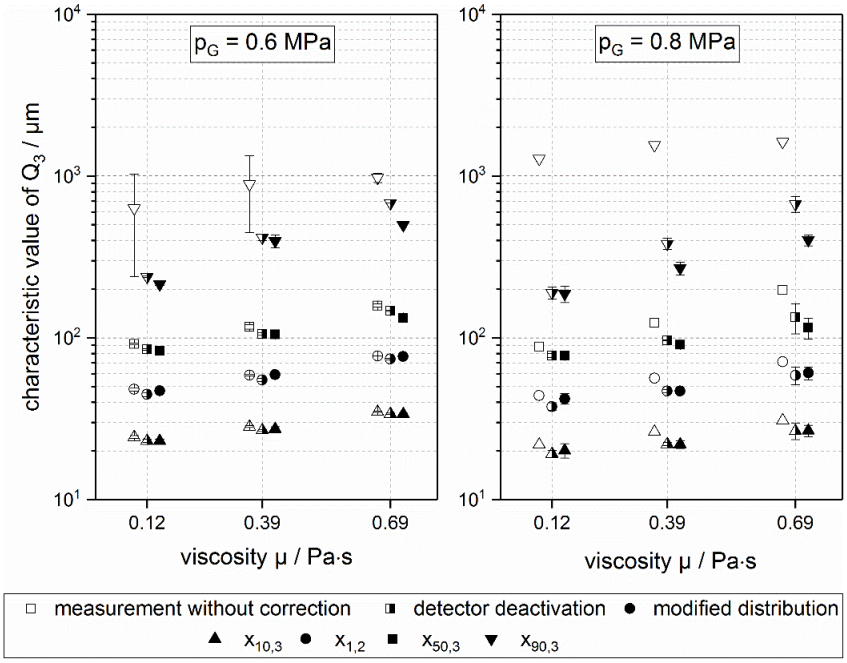

Figure 9. Characteristic values ($x_{10,3}$, $x_{50,3}$, $x_{90,3}$, $\overline{x}_{1,2}$) of droplet size distributions, corrected by the method of detector deactivation (Det. off, empty symbols) and the new modification procedure (Mod., filled symbols) at different viscosities (0.12, 0.39, 0.69 Pa·s) and gas pressures of 0.6 MPa (**left**) and 0.8 MPa (**right**).

As would be expected, larger droplets and wider droplet size distributions, represented by larger differences between $x_{10,3}$ and $x_{90,3}$ values, are generated with increasing liquid viscosity. At both applied gas pressures (0.6 and 0.8 MPa) each characteristic value ($x_{10,3}$, $x_{50,3}$, $x_{90,3}$, $\overline{x}_{1,2}$) increases significantly ($p < 0.05$) with increasing viscosity (0.12, 0.39, 0.69 Pa·s), independently of the handling of the beam-steering effect. Comparing the results at the same viscosity, characteristic values decrease significantly with increasing gas pressure, with the exception of uncorrected $x_{90,3}$ values (measurement without correction) at viscosities of 0.39 and 0.69 Pa·s.

Comparing values of the measurement without correction to corrected values, at the same viscosity and a gas pressure of 0.8 MPa, all corrected values are significantly smaller than uncorrected ones, independently of the used correction method. When a gas pressure of 0.6 MPa is applied, this is only the case for values of $x_{90,3}$.

When results of the two different correction methods are compared to each other at the same viscosities and gas pressures, $x_{90,3}$ values of the new modification method are significantly smaller than the ones generated by detector deactivation. Exceptions include the results at a gas pressure of 0.6 MPa and a viscosity of 0.39 Pa·s, as well as the results at a gas pressure of 0.8 MPa and a viscosity of 0.12 Pa·s. In these cases, no significant differences are found between the $x_{90,3}$ values of the two methods. Also for all other characteristic values ($x_{10,3}$, $x_{50,3}$, $\overline{x}_{1,2}$), no significant differences between the results of both methods are found.

As a consequence, the presented modification method should be applied in spray droplet size measurements when beam steering occurs and the largest droplets of a distribution have an over-proportional impact on the stability and performance of a subsequent process step. This is the case in complex processes, like spray drying, spray painting, or combustion. In turn, the method of detector deactivation shows excellent agreement when the real and apparent parts of the measured droplet size distribution can be clearly separated from each other. Hence, this method can still be used safely for beam-steering correction in the case of separated distribution parts.

4. Conclusions

In the presented study, a new correction method for the beam-steering effect is presented. The beam-steering effect is a systematic error, occurring in laser diffraction measurements of spray droplet sizes, generated by pneumatic atomization or when parts of the liquid phase evaporate in the measurement zone. Due to this measurement error, apparent large droplets are detected, leading to a misbalance in the measured size distributions. This misbalance is problematic if the results of the performed droplet size measurements are used in the design of subsequent process steps which are over-proportionally influenced by large droplets.

The commonly used method for correction of the beam-steering effect is based on a reduction of the measurement range of the used laser diffraction device by detector deactivation. This method is applicable when real droplet sizes are clearly smaller than apparent droplet sizes, caused by the beam-steering effect. If the real and apparent parts of the distribution overlap, some detectors cannot be deactivated without cutting the real droplet size distribution. As a consequence, an overestimation of large droplets has to be accepted when detector deactivation is applied. However, the method of detector deactivation shows excellent results when real and apparent droplet sizes are completely separated. Therefore, this method can still be used safely in the case of separated distribution parts.

The presented correction method is based on a multimodal log-normal fit of measured distributions. The modality, representing the largest droplets was assumed to be caused by the beam-steering effect. This assumption was verified by measurements without liquid droplets. The real size distribution is calculated by splitting the beam-steering modality from the measured distribution.

The new method was applied to previously published droplet size measurements, using an internal mixing ACLR atomizer, which had not yet been analyzed according to the largest droplets of the distribution. In measurements with overlapping real and apparent size distributions, the new method clearly reduced the overestimation of large droplets in measured size distributions, compared to results of the method of detector deactivation. The method can be applied to all tested measurement scenarios and seems to be valid for all spray droplet size measurements by laser diffraction. Therefore, the new modification method is recommended for use in all laser diffraction measurements of spray droplets, in which the beam-steering effect occurs.

Author Contributions: Conceptualization, M.O.W. and V.G.; Methodology, M.O.W.; Validation, M.O.W., H.P.K. and V.G.; Investigation, M.O.W.; Writing-Original Draft Preparation, M.O.W.; Writing-Review & Editing, H.P.K. and V.G.; Visualization, M.O.W.; Funding Acquisition, H.P.K. and V.G.

Funding: The IGF Project AiF 18299 N of the FEI was supported via AiF within the programme for promoting the Industrial Collective Research (IGF) of the German Ministry of Economic Affairs and Energy (BMWi), based on a resolution of the German Parliament.

Acknowledgments: We acknowledge support by Deutsche Forschungsgemeinschaft and Open Access Publishing Fund of Karlsruhe Institute of Technology. The authors further express their thanks to Sabine Schneider, Sabine Mizera, and Andrea Butterbrodt for experimental support.

Conflicts of Interest: The authors declare no conflict of interest. The funders had no role in the design of the study; in the collection, analyses, or interpretation of data; in the writing of the manuscript, and in the decision to publish the results.

References

1. Lefebvre, A.H. *Atomization and Sprays*; Taylor & Francis: Bristol, PA, USA, 1989.
2. Black, D.L.; McQuay, M.Q.; Bonin, M.P. Laser-based techniques for particle-size measurement: A review of sizing methods and their industrial applications. *Prog. Energy Combust.* **1996**, *22*, 267–306. [CrossRef]
3. Dumouchel, C.; Yongyingsakthavorn, P.; Cousin, J. Light multiple scattering correction of laser-diffraction spray drop-size distribution measurements. *Int. J. Multiphase Flow* **2009**, *35*, 277–287. [CrossRef]
4. Dodge, L.G.; Cerwin, S.A. Extending the Applicability of Diffraction-Based Drop Sizing Instruments. *Liq. Part. Size Meas. Tech.* **1984**, 72–81. [CrossRef]
5. Mescher, A.; Walzel, P. Störeinfluss durch Schlieren bei der Tropfengrößenmessung an Zweistoffdüsen durch Laserbeugungsspektrometrie. *Chem. Eng. Technol.* **2010**, *82*, 717–722. [CrossRef]

6. Chigier, N. Comparative Measurements Using Different Particle Size Instruments. *Liq. Part. Size Meas. Tech.* **1984**, 169–186. [CrossRef]
7. Miller, B.V.; Lines, R.W. Recent Advances in Particle Size Measurements: A Critical Review. *Crit. Rev Anal. Chem.* **1988**, *20*, 75–116. [CrossRef]
8. Swithenbank, J.; Beer, J.; Taylor, D.; Abbot, D.; McCreath, G. A laser diagnostic technique for the measurement of droplet and particle size distribution. In Proceedings of the 14th Aerospace Sciences Meeting, Washington, DC, USA, 26–28 January 1976; American Institute of Aeronautics and Astronautics: Washington, DC, USA, 1976.
9. Bernhardt, C. *Particle Size Analysis: Classification and Sedimentation Methods*; Springer Netherlands: Dordrecht, The Netherlands, 1994.
10. Dzubay, T.G.; Hasan, H. Fitting Multimodal Lognormal Size Distributions to Cascade Impactor Data. *Aerosol. Sci. Technol.* **1990**, *13*, 144–150. [CrossRef]
11. Tropea, C.; Yarin, A.L.; Foss, J.F. (Eds.) *Springer Handbook of Experimental Fluid Mechanics*; Springer: Berlin/Heidelberg, Germany, 2007.
12. Settles, G.S.; Hargather, M.J. A review of recent developments in schlieren and shadowgraph techniques. *Meas. Sci. Technol.* **2017**, *28*, 42001. [CrossRef]
13. Malvern Instruments Ltd. *Spraytec User Manual Man 0368*; Malvern Instruments Ltd.: Malvern, UK, 2007.
14. Wittner, M.O.; Karbstein, H.P.; Gaukel, V. Spray performance and steadiness of an effervescent atomizer and an air-core-liquid-ring atomizer for application in spray drying processes of highly concentrated feeds. *Chem. Eng. Process.* **2018**, *128*, 96–102. [CrossRef]
15. Stähle, P.; Gaukel, V.; Schuchmann, H.P. Comparison of an Effervescent Nozzle and a Proposed Air-Core-Liquid-Ring (ACLR) Nozzle for Atomization of Viscous Food Liquids at Low Air Consumption. *J. Food Process Eng.* **2017**, 40. [CrossRef]
16. Stähle, P.; Schuchmann, H.P.; Gaukel, V. Performance and Efficiency of Pressure-Swirl and Twin-Fluid Nozzles Spraying Food Liquids with Varying Viscosity. *J. Food Process Eng.* **2017**, *40*. [CrossRef]
17. Kleinhans, A.; Georgieva, K.; Wagner, M.; Gaukel, V.; Schuchmann, H.P. On the characterization of spray unsteadiness and its influence on oil drop breakup during effervescent atomization. *Chem. Eng. Process.* **2016**, *104*, 212–218. [CrossRef]
18. Kleinhans, A.; Hornfischer, B.; Gaukel, V.; Schuchmann, H.P. Influence of viscosity ratio and initial oil drop size on the oil drop breakup during effervescent atomization. *Chem. Eng. Process.* **2016**, *109*, 149–157. [CrossRef]